Amplitude and Frequency Modulation Distortions of a Loudspeaker*

HIDEO SUZUKI** AND SHIGENORI SHIBATA

Mitsubishi Electric Corporation, Consumer Products Research Laboratory, Kamakura, Kanagawa, Japan

The measurement techniques and the causes of amplitude and frequency modulation distortions are discussed using a two-way coaxial-type loudspeaker system. The distortion due to amplitude modulation is caused by the dependence of the radiation efficiency of the high-frequency driver on the displacement of the diaphragm of the low-frequency driver. The distortion due to frequency modulation seems to be produced when the high-frequency sound has a nonzero particle velocity in the axis direction at the surface of the low-frequency driver diaphragm. The symmetry of the sidebands of the summed modulation distortion (intermodulation distortion) indicates that the amplitude and frequency modulation distortions are 90° out of phase with each other.

0 INTRODUCTION

It is well known that a high-frequency signal is modulated by a low-frequency signal when they are fed into a single driver or a multiway loudspeaker system. In this case both the amplitude and the frequency of the high-frequency component are modulated, although the magnitudes of these modulations are highly dependent on the type of loudspeaker. Many studies have been conducted on the frequency modulation distortion (FMD) and some on the amplitude modulation distortion (AMD). Beers and Belar seem to have performed the original study on the FMD of a loudspeaker, presenting equations to predict the magnitude of FMD [1]. Klipsch published a series of papers [2]–[4] discussing the differences of the amount of AMD and FMD between the direct-radiator type and the horn-type loudspeakers, and their effect on the quality of the reproduced sound. Moir discussed the Doppler distortion of loudspeakers with different diameters, and also presented a technique to measure FMD using music and speech sources [5]. Kurtin proposed a simple quantitative index of FMD as a criterion in the design of loudspeaker studies [6].

In spite of these excellent works, several important questions about AMD and FMD remain as yet unsolved. Those are:

1) A complete model (or formula) to predict the amount of AMD and FMD of a single loudspeaker or a multiway system has not been given.

2) The cause of AMD is assumed (mostly without verification) to be the nonlinear distortion of a loudspeaker in the low-frequency region.

3) The phase relationships between AMD and FMD are not known.

4) The directional characteristics or the total radiated power of the modulation distortions are not well investigated.

In this paper, with these questions in mind, both the AMD and the FMD of the coaxial-type loudspeaker with a flat diaphragm are discussed. The most emphasis is placed on the discussion of the causes of these distortions.

1 LOUDSPEAKER USED FOR TEST

Fig. 1 shows the cross section of the coaxial-type loudspeaker system used for this study. The low-frequency driver (woofer) has a ring-shaped flat diaphragm which consists of two outer layers of carbon-fiber-reinforced plastic and an aluminum honeycomb core. The inner and outer radii of the diaphragm are 120 and 220 mm, respectively. The high-frequency driver (tweeter) is a conventional 50-mm cone-type tweeter which is located at the center of the woofer. An enclosure with a very large baffle was used so that the assumption of an infinite baffle boundary condition is assured over

* Presented at the 74th Convention of the Audio Engineering Society, New York, 1983 October 8–12.

** Present address: CBS Technology Center, Stamford, CT 06905, USA.

2.2 Discussion

A possible reason for the generation of AMD is that the radiation efficiency of the tweeter is modified by the (static) position of the woofer's diaphragm. The AMD obtained from this assumption will be compared with the measured AMD in order to test the validity of the assumption.

Applying a 10-V input to the woofer resulted in an amplitude of 4.7 mm peak to peak. The relation between the position of the woofer diaphragm and the applied dc current is shown in Fig. 6. With this relationship the diaphragm of the woofer can be statically positioned anywhere by adjusting the dc current. The effect of the position of the woofer diaphragm on the tweeter's on-axis sound pressure measured at 1 m from the system is shown in Fig. 7. Fig. 7 shows that the on-axis sound pressure of the high-frequency unit is significantly affected by the position of the woofer diaphragm. Fig. 7 also shows that it is highly frequency dependent, and it has positive or negative slopes, or parabolic shapes, depending on frequency ω_2. From this figure the amount of AMD can be predicted as follows. The sound pressure of the tweeter can be expressed by

$$P_2(t) = f(x) \cos \omega_2 t \tag{1}$$

where $f(x)$ is the amplitude of the tweeter, which is dependent on the position of the diaphragm of the woofer. Actually the curves shown in Fig. 7 are examples of the function $f(x)$ when $f(x)$ is expressed in decibels with the reference amplitude at $x = 0$. If x changes as a function of time with frequency ω_1, the function $f(x)$ can be expressed as a function of time with the same frequency. Then it can be expanded as a Fourier series, such as

$$f(t) = \frac{a_0}{2} + \sum_{k=1}^{\infty} a_k \cos (k\omega_1 t + \theta_k) \tag{2}$$

where a_k is the Fourier coefficient. Substituting Eq. (2) into Eq. (1), we have

$$\begin{aligned} P_2(t) &= \frac{a_0}{2} [1 + A_1 \cos (\omega_1 t + \theta_1) \\ &\quad + A_2 \cos (2\omega_1 t + \theta_2) + \cdots] \cos \omega_2 t \\ &= \frac{a_0}{2} \left\{ 1 + \frac{A_1}{2} [\cos\{(\omega_2 - \omega_1)t - \theta_1 \right. \\ &\quad + \cos(\omega_2 + \omega_1)t + \theta_1\}] \\ &\quad + \frac{A_2}{2} [\cos(\omega_2 - 2\omega_1)t - \theta_2 \\ &\quad \left. + \cos(\omega_2 + 2\omega_1)t + \theta_2] + \cdots \right\} \end{aligned} \tag{3}$$

with $A_k = 2a_k/a_0$.

It is obvious that if $f(x)$ = constant, all the coefficients except a_0 are zero and no distortion is generated. If

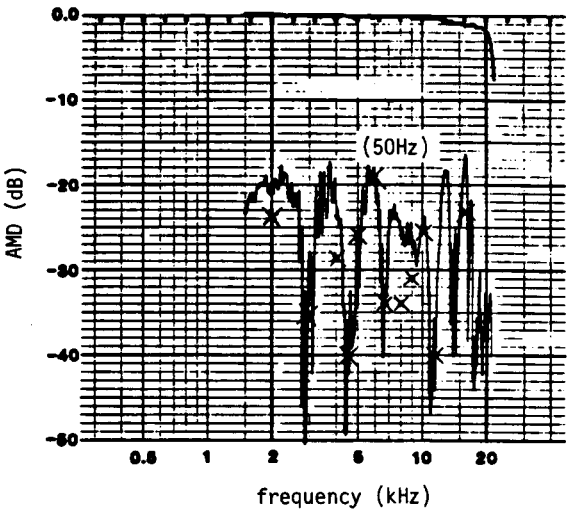

Fig. 4. AMD of 50-Hz components. ×—estimated AMDs from Fig. 7.

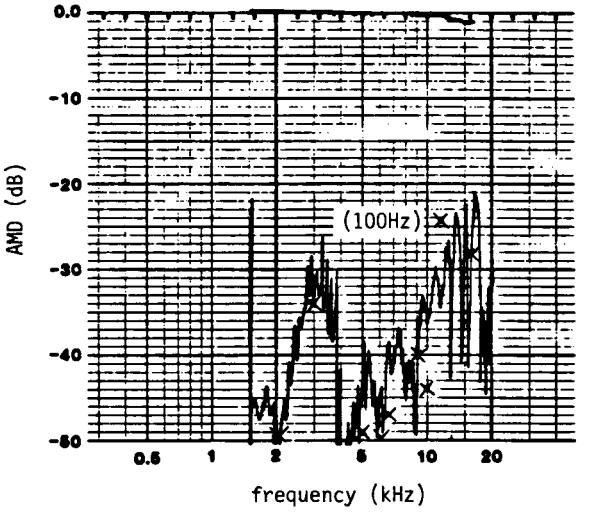

Fig. 5. AMD of 100-Hz components. ×—estimated AMDs from Fig. 7.

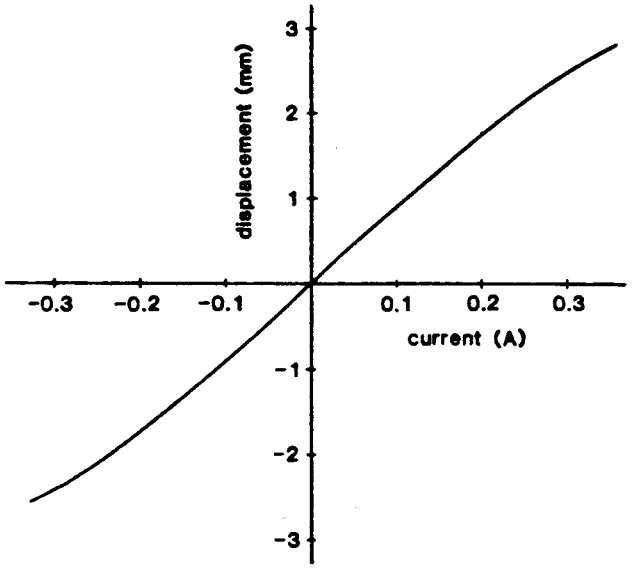

Fig. 6. Relation between static displacement of woofer diaphragm and input dc current.

the frequency range of interest (1.5–20 kHz). A very simple configuration of this system was convenient for the analysis of AMD and FMD.

2 AMPLITUDE MODULATION DISTORTION (AMD)

2.1 Measurement Technique and Results

A block diagram of the system for measuring AMD and FMD is shown in Fig. 2. The low-frequency (ω_1) and high-frequency (ω_2) components are generated by oscillators 1 and 2, respectively, and the amplified outputs are applied to the low- and high-frequency units individually. The sound output picked up by the microphone contains a low-frequency component and an amplitude- and frequency-modulated high-frequency component. The low-frequency component is rejected by the high-pass filter. In the measurement of AMD and FMD, the output of the high-pass filter was used as a compressor input to oscillator 2 so that the high-frequency sound output remains constant.

The AMD component can be obtained by any type of amplitude detection method. In the present study a half-wave rectification was used as the detector. Generally the rectified signal consists of a dc component, the low-frequency components (ω_1, $2\omega_1$, . . .), and the high frequency components (ω_2, $2\omega_2$, . . .). AMD is analyzed by a narrow band-pass filter, and each component with frequency ω_1, $2\omega_1$, . . . is recorded on a chart using a level recorder, which is synchronized with oscillator 2. Comparison of the level with the ω_2 component gives the degree of distortion.

An amplitude-modulated wave of the form $(1 + A \cos \omega_1 t) \cos \omega_2 t$ was rectified and used with the experimental apparatus in Fig. 2. The result was obtained as the relation between A and the level difference between ω_1 and ω_2 components. This relation is shown in Fig. 3. For example, if the level difference is −18 dB, A is equal to 0.2. This corresponds to −20 dB of AMD if the distortion is expressed by 20 log (A/2). The frequency and the input level of the low-frequency component were kept constant at 50 Hz and 10 V, respectively. The input level of the high-frequency component was adjusted so that the on-axis sound-pressure level at 1 m remained constant at 90 dB.

The results are shown in Figs. 4 and 5 for 50-Hz and 100-Hz components, respectively. The peak levels of the 50-Hz component are about −20 dB when AMD is represented by 20 log (A/2), showing high modulation distortions over the entire range from 1.5 to 20 kHz. The 100-Hz component is much smaller than the 50-Hz component, and shows large values around 3 kHz and 15 kHz. The relatively large values of distortion compared with regular two-way systems come from the fact that the low- and high-frequency units are very close to each other. It should be noted that even a woofer with a flat diaphragm does not reduce AMD significantly. The higher frequency distortion components are not shown because they were much smaller than the first two components.

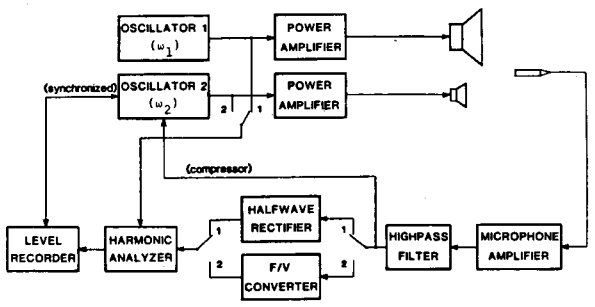

Fig. 2. Measuring system of AMD and FMD.

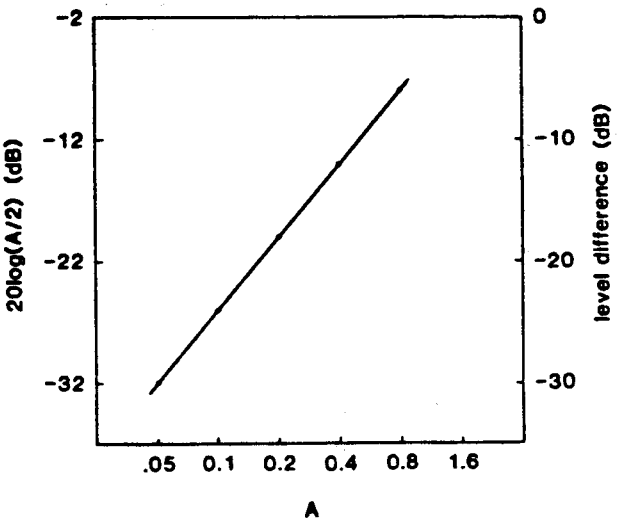

Fig. 3. Relation between A and the level difference of the ω_1 and ω_2 components of the rectified signal of $(1 + A \cos \omega_1 t) \cos \omega_2 t$.

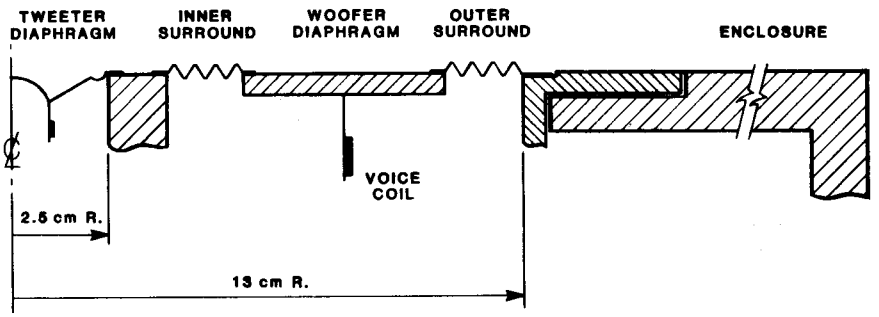

Fig. 1. Geometry of coaxial loudspeaker system used for experiment.

with respect to time, such as

$$\omega(t) = \omega_2 + \phi_m\omega_1 \cos \omega_1 t \ . \quad (5)$$

The output of the frequency–voltage converter is given by

$$V = K(\omega_2 + \phi_m\omega_1 \cos \omega_1 t) \quad (6)$$

where K is the converting constant of a specific converter. Then from the level of the band-pass output ΔV (0 to peak), the modulation index is given by

$$\phi_m = \frac{\Delta V}{K\omega_1} \ . \quad (7)$$

Eq. (4) is rewritten as follows [7]:

$$P_2 = C\left\{\cos \omega_2 t + \frac{\phi_m}{2}[\cos (\omega_2 - \omega_1)t - \cos (\omega_2 + \omega_1)t]\right\} \quad (8)$$

where the higher order components of the sideband were neglected by assuming that $\phi_m << 1$ (this is almost always valid for the real case). Now FMD can be represented in decibels, such as 20 log $(\phi_m/2)$.

The results are shown in Fig. 8. The input frequency and voltage to the woofer were 50 Hz and 10 V, respectively. The output of the high-frequency unit was kept constant at 90 dB, while the frequency was changed from 1 kHz to 15 kHz. The highest level of FMD is about −20 dB, which is almost the same with AMD. Wide peaks are observed around 1.5, 3.0, 6.6, and 12 kHz, which are almost in equal ratios with each other. It is not clear if there is any significance in this fact.

For comparison, the upper $(\omega_2 + \omega_1)$ and lower $(\omega_2 - \omega_1)$ components of the total modulation distortion measured using a B&K distortion measurement control unit (type 1902) are shown in Fig. 9. (In this measurement the input voltage to the tweeter was kept constant at 2.8 V.) It can be said that both the upper and the lower components are almost identical. The symmetry of the intermodulation distortion will be discussed later

3.2 Near-Field Measurement of FMD

It is necessary to know how and where FMD is generated, if any reduction is intended. FMD in the near field was measured for this reason. The frequencies used were 1.5, 3.0, and 6.6 kHz, where the large FMDs were observed in the previous measurement. The absolute values of the FMD component [$C\phi_m/2$ in Eq. (8)] were obtained along the surface of the loudspeaker system, and they were normalized so that a maximum value became equal to unity. The results are shown in Fig. 10. The figure includes the cross section of the loudspeaker system, where the measurement points along the surface are indicated by arrows. The FMD is largest at the center for 1.5 kHz, but maximum points are also seen on the inner surround for 3.0 and 6.6 kHz. All three curves show peaks on the inner and outer surrounds. These results indicate that FMD is mostly generated on the area where the surface is not flat. When the high-frequency (ω_2) sound propagates along the surface of the woofer, it has a nonzero component normal to the surface on the inner and outer surrounds. This component will contribute to the generation of FMD when the woofer is driven back and forth with frequency ω_1, due to the Doppler effect. In other words, FMD is produced where the diaphragm of the woofer works as a secondary source of the high-frequency sound.

3.3 Directivity Pattern of FMD

It is important to know the directivity pattern of FMD since it gives a clue to the location of the source and it also gives the radiated power in 2π free space. The

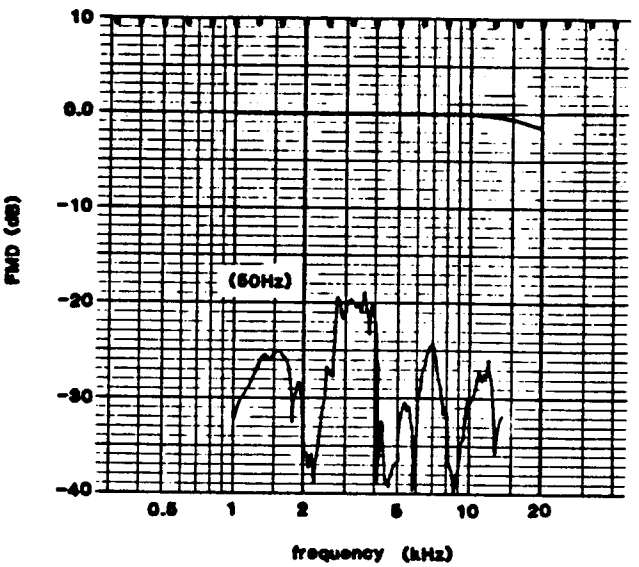

Fig. 8. FMD of 50-Hz component.

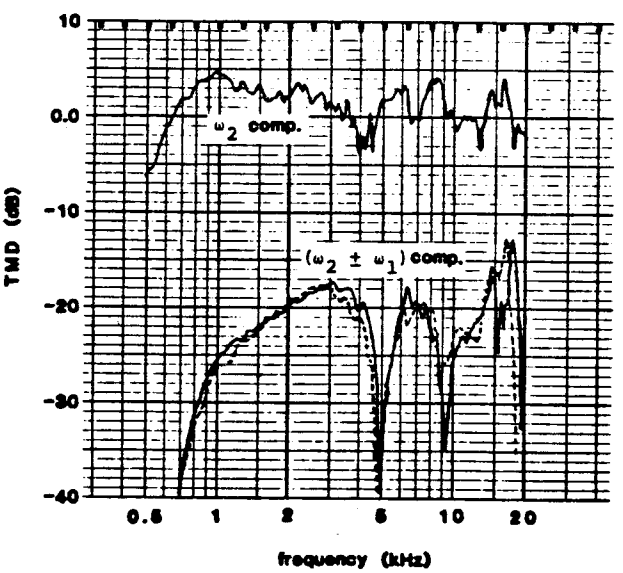

Fig. 9. Total modulation distortion of upper (solid line) and lower (dotted line) components $\omega_2 \pm 50$ Hz.

$f(x)$ is linear, such as $f(x) = Ax + B$, then a_0 and a_1 are nonzero and only distortion components with frequencies $(\omega_2 \pm \omega_1)$ are generated. If $f(x) = Ax^2 + B$, then $(\omega_2 \pm 2\omega_1)$ components are generated.

From Fig. 7, 20 log $(A_1/2)$ and 20 log $(A_2/2)$ were calculated and plotted in Figs. 4 and 5, respectively. The agreement between measured and calculated AMDs for both the 50-Hz and the 100-Hz components is good, although large discrepancies are observed at some freuquencies. This agreement shows that AMD is caused by the fact that the radiation efficiency of the tweeter is influenced by the position of the woofer diaphragm. Fig. 7 shows that the level of each component of the sideband is significant up to second order (that is, $\omega_2 \pm 2\omega_1$), since the functions in Fig. 7 may be approximated by the form $f(x) = Ax^2 + Bx + C$.

The above conclusion indicates that if the surrounds were made of flat flexible rings rather than the V-shaped rings, the AMD would be smaller, since a smoother boundary has a smaller effect on the radiation efficiency of the tweeter.

3 FREQUENCY MODULATION DISTORTION (FMD)

3.1 Measurement Technique and Results

The measurement technique of FMD is almost the same as that of AMD. A difference exists only in the detection process. The frequency detection is easily accomplished using a frequency–voltage converter. When a frequency-modulated carrier is given to the frequency–voltage converter, it produces a voltage output comprised of a dc component corresponding to frequency ω_2 and an ac component with the modulation frequency ω_1 and its harmonics. Using a low-frequency band-pass filter, FMD can be measured. This process is described as follows. Assume that the frequency-modulated signal is simply expressed by

$$P_2 = C \cos(\omega_2 t + \phi_m \sin \omega_1 t) \quad (4)$$

where ϕ_m is the modulation index. The instantaneous frequency is obtained by differentiating the phase term

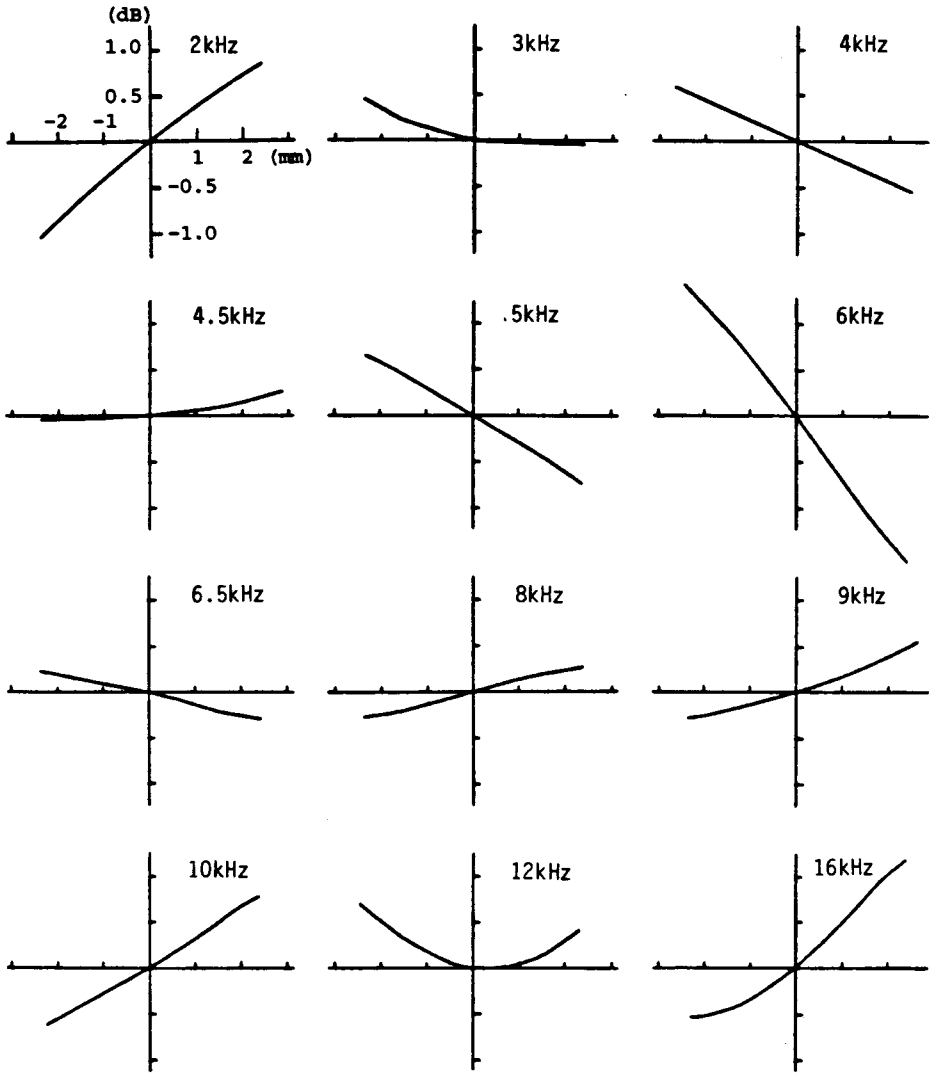

Fig. 7. Dependence of on-axis sound pressure of tweeter at 1 m on position of woofer diaphragm. Scales of axes are the same for all frequencies.

solid line in Fig. 11 shows the directivity pattern of FMD at 1.5 kHz. The right-hand side and left-hand side patterns are not completely symmetric, but show roughly the same width. The solid lines in Figs. 12 and 13 are the measured directivity patterns at 3 kHz and 6.6 kHz (right-hand side only), respectively. In general the directivity patterns are much sharper than those of the tweeter itself at the corresponding frequencies.

The dotted lines (except the left-hand side of Fig. 11) are the directivity patterns calculated using the following assumptions:

1) The inner and the outer surrounds are the sources of FMD.

2) The velocity ratio of the inner and outer surrounds as sound sources is the ratio of the measured FMD levels on the inner and outer surrounds (see Fig. 10).

3) The velocities of the inner and outer surrounds are in phase (since both surrounds vibrate in phase).

The agreement between measured and calculated directivity patterns is very good for 3.0 and 6.6 kHz. At 1.5 kHz the directivity pattern calculated from the above three assumptions is much wider than the measured pattern. The dotted line of the left-hand side of Fig. 11 shows the pattern when only the outer surround is considered. This pattern shows a much better agreement with the measurement. A trend is seen that as the frequency decreases, the outer surround becomes more effective as a secondary source.

The above discussion confirms the result obtained from the near-field measurement that the nonflat part of the diaphragm of the low-frequency unit is the major contributor to the generation of FMD.

3.4 Symmetry of Sidebands

The upper and lower sidebands of AMD or FMD are symmetric, as shown in Eq. (3) or Eq. (8). When they exist together, however, their symmetry is not necessarily guaranteed. If we assume that $A_1 = \phi_m$ and $\theta_1 = 0$ in Eqs. (3) and (8), the first-order upper sidebands of AMD and FMD cancel each other. The same thing happens for the lower sidebands when $\theta_1 = \pi$. The AMD and FMD components must be 90° out of phase in order for the total intermodulation distortion to be symmetric. As Fig. 7 shows, the modulated component of the amplitude of the high-frequency sound is mostly proportional to the displacement of the woofer diaphragm. Then, approximately, the amplitude-modulated sound pressure can be expressed as

$$P_{AM} = (1 + A \sin \omega_1 t) \cos \omega_2 t$$

$$= \cos \omega_2 t + \frac{A}{2} [\sin(\omega_2 + \omega_1)t - \sin(\omega_2 - \omega_1)t] \quad (9)$$

where the phase was chosen such that the amplitude of the woofer becomes zero when $t = 0$. On the other hand, the maximum frequency of the high-frequency component corresponds to the time when the velocity of the woofer diaphragm is maximum. Therefore the frequency-modulated sound pressure should be expressed as

$$P_{FM} = \cos (\omega_2 t + \phi_m \sin \omega_1 t)$$

$$= \cos \omega_2 t + \frac{\phi_m}{2} [\cos (\omega_2 + \omega_1)t - \cos (\omega_2 - \omega_1)t] . \quad (10)$$

The sidebands of the above two equations are 90° out of phase, and they do not cancel each other even if $A = \phi_m$.

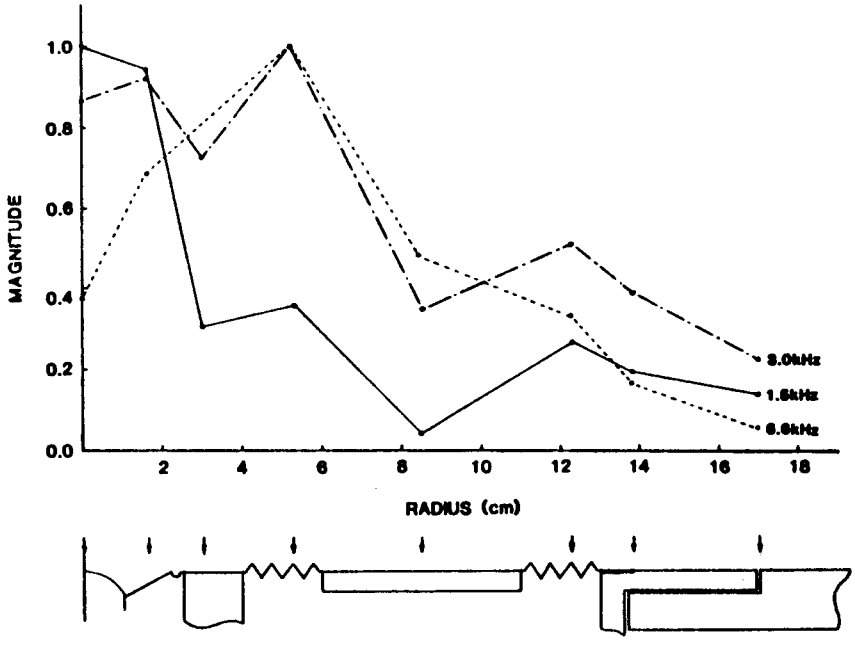

Fig. 10. Near-field distribution of FMD.

Thus if we assume that the amplitude-modulated term of the high-frequency component is proportional to the displacement of the woofer, and that the frequency-modulated term is proportional to the velocity of the diaphragm of the low-frequency unit, the symmetry of the sidebands is preserved. Of course, if either AMD or FMD is much greater than the other, the symmetry is also preserved.

4 CONCLUSION

The AMD and the FMD of a coaxial-type loudspeaker system were discussed. In this particular case both distortions have the same order of magnitude, and neither of them should be neglected in the discussion of the total modulation distortion. It was found that AMD is generated because the radiation efficiency of the tweeter is affected by the diplacement of the woofer diaphragm (including the surround). This was shown by the measurement of the change of the on-axis sound pressure of the tweeter caused by the change of the static displacement of the woofer diaphragm.

Locating the source of FMD was investigated by measuring the near-field distribution and the directivity characteristics of the distortion. Both measurements confirmed that FMD is produced mostly on the inner and outer surrounds, which are the nonflat portions of the vibrating system of the woofer. The phase relationship between AMD and FMD was discussed in conjunction with the symmetry of the upper and lower sidebands.

The coaxial-type loudspeaker used for this study is not a typical one, and some of the conclusions might be different if another type of loudspeaker was used. It is hoped, however, that the techniques of measurement

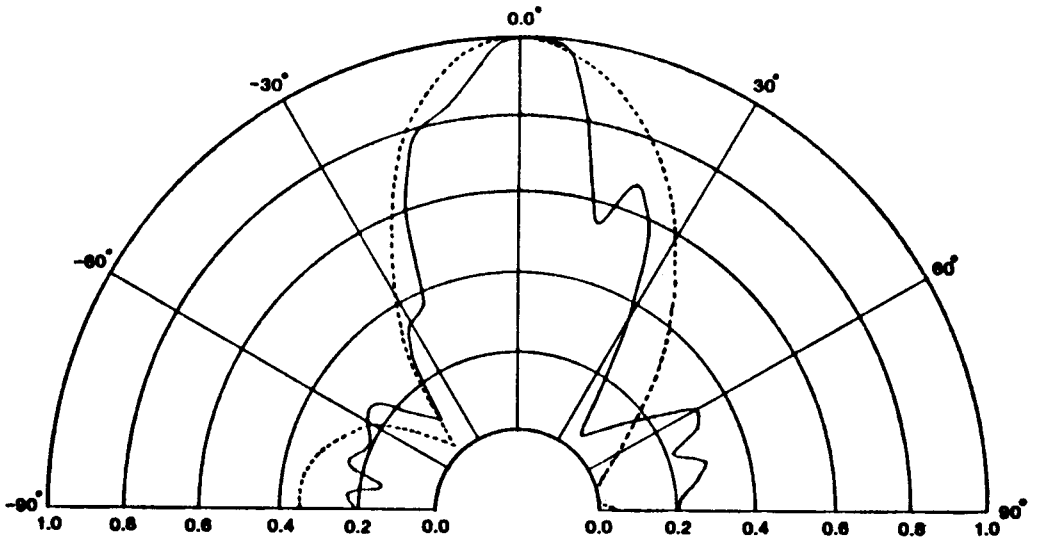

Fig. 11. Measured (solid line) and calculated (dotted line) directivity patterns of FMD at 1.5 kHz. Dotted line of right-hand side—directivity pattern of double-ring source; dotted line of left-hand side—directivity pattern of single-ring source (outer surround only).

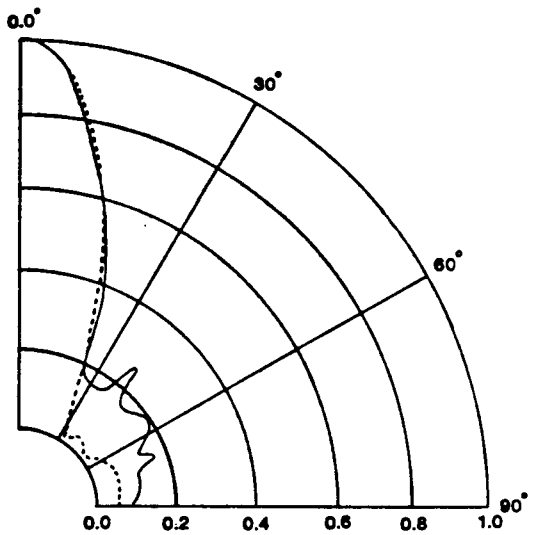

Fig. 12. Measured (solid line) and calculated (dotted line) directivity patterns of FMD at 3 kHz.

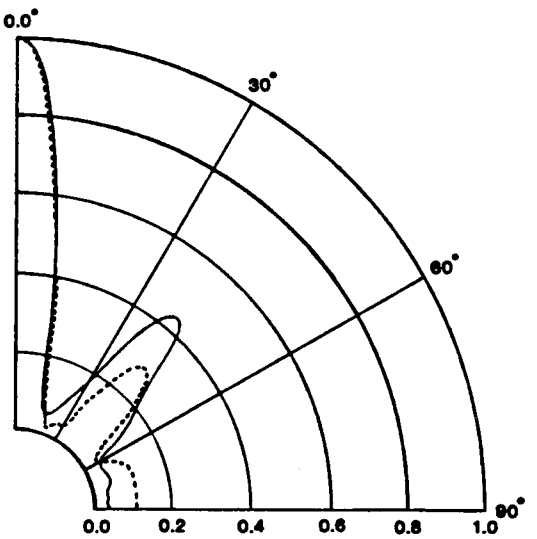

Fig. 13. Measured (solid line) and calculated (dotted line) directivity patterns of FMD at 6.6 kHz.

and analysis described here are general and can be applied to other problems.

5 ACKNOWLEDGMENT

The authors wish to express their graditude to the persons in the Loudspeaker Research Group at the Consumer Products Research Laboratory, Mitsubishi Electric Corporation, who have contributed greatly to the discussion of this study. The authors are also thankful for the support and the encouragement given by Dr. Takeo Shindo, who was the Director of the R&D Department when this study was performed.

6 REFERENCES

[1] G. L. Beers and H. Belar, "Frequency-Modulation Distortion in Loudspeakers," *Proc. IRE*, vol. 31, pp. 132–138 (1943 Apr.).

[2] P. W. Klipsch, "Modulation Distortion in Loudspeakers," *J. Audio Eng. Soc.*, vol. 17, pp. 194–206 (1969 Apr.).

[3] P. W. Klipsch, "Modulation Distortion in Loudspeakers: Part II," *J. Audio Eng. Soc.*, vol. 18, pp. 29–33 (1970 Feb.).

[4] P. W. Klipsch, "Modulation Distortion in Loudspeakers: Part III," *J. Audio Eng. Soc.*, vol. 20, pp. 827–828 (1972 Dec.).

[5] J. Moir, "Doppler Distortion in Loudspeakers," *Audio*, vol. 60, no. 8, pp. 42–52 (1976).

[6] S. Kurtin, "Frequency Modulation in Loudspeakers as a Loudspeaker Design Criterion," *Audio*, vol. 61, no. 12, pp. 52–57 (1977).

[7] J. B. Thomas, *Statistical Communications Theory* (Wiley, New York, 1969).

THE AUTHORS

H. Suzuki

S. Shibata

Hideo Suzuki has been a senior acoustical engineer at the CBS Technology Center since mid-1981, following the completion of the doctoral program in acoustics at Pennsylvania State University. He previously studied electrical engineering at Tohoku University in Japan, obtaining B.S. and M.S. degrees. From 1967 to 1979, he worked for Mitsubishi Electric Corporation in the area of loudspeaker development and research.

At the CBS Technology Center, Dr. Suzuki is engaged in the vibration and sound radiation analysis of musical instruments, loudspeaker development, and in some other acoustics-related areas. He published several papers in loudspeaker research in the JAES, JASA, and JASJ. He is a member of the AES and the ASA.

•

Shigenori Shibata was born in Toyama Prefecture, Japan. After graduating from Toyama Technical High School in 1969, he began working in the Consumer Products Research Laboratory at Mitsubishi Electric Corporation in the field of computer-aided design of induction motors. Since 1974, he has been involved in the research and development of loudspeakers as an electrical engineer.